AGU ADVANCING EARTH AND SPACE SCIENCES

JGR Oceans

RESEARCH ARTICLE
10.1029/2025JC022956

Sensitivity of Flood Extent and Population Exposure to Variations in Bathymetry Across a Shallow Continental Shelf Lagoon

Zaid Al-Attabi[1,2], Siddharth Narayan[1], Anthony Campbell[3,4], Ananth Wuppukondur[1,5], Daystar Babanawo[1], Yicheng Xu[1], Nathan Thomas[3,6], Lola Fatoyinbo[3], and David Lagomasino[1]

[1]Department of Coastal Studies, Integrated Coastal Programs, East Carolina University, Wanchese, NC, USA, [2]Department of Marine Sciences, Marine Sciences Center, University of Basrah, Basrah, Iraq, [3]NASA Goddard Space Flight Center, Greenbelt, MD, USA, [4]Goddard Earth Sciences Technology and Research (GESTAR) II, University of Maryland, Baltimore, MD, USA, [5]Department of Civil Engineering, MNNIT Allahabad, Allahabad, India, [6]Department of History, Geography and Social Sciences, Edge Hill University, Ormskirk in Lancashire, UK

Key Points:

- Deeper lagoons result in lower coastal flooding and population exposure, except in enclosed lagoons with median depths less than <2 m
- Vertical bathymetric uncertainties can vary flood extent estimates by up to 12%
- New open-access satellite-derived data set for Belize nearshore bathymetry includes vertical uncertainties

Supporting Information:

Supporting Information may be found in the online version of this article.

Correspondence to:

Z. Al-Attabi,
zrahman@geol.sc.edu

Citation:

Al-Attabi, Z., Narayan, S., Campbell, A., Wuppukondur, A., Babanawo, D., Xu, Y., et al. (2026). Sensitivity of flood extent and population exposure to variations in bathymetry across a shallow continental shelf lagoon. *Journal of Geophysical Research: Oceans*, *131*, e2025JC022956. https://doi.org/10.1029/2025JC022956

Received 30 MAY 2025
Accepted 28 JAN 2026

Author Contributions:

Conceptualization: Zaid Al-Attabi, Siddharth Narayan, David Lagomasino
Data curation: Zaid Al-Attabi, Anthony Campbell, Daystar Babanawo
Formal analysis: Zaid Al-Attabi, Siddharth Narayan
Funding acquisition: Zaid Al-Attabi, Siddharth Narayan, Anthony Campbell, Lola Fatoyinbo, David Lagomasino
Investigation: Zaid Al-Attabi
Methodology: Zaid Al-Attabi, Siddharth Narayan, Anthony Campbell, David Lagomasino
Project administration: Zaid Al-Attabi, Siddharth Narayan, Anthony Campbell
Resources: Zaid Al-Attabi, Siddharth Narayan

Abstract

Bathymetry is a critical input to storm surge models on coastlines fronted by lagoon systems, yet few studies explore how variations in bathymetry influence flood impacts, flooded extent, and exposed population across these globally widespread morphologies. Here, we investigate the influence of variations in bathymetry on storm inundation impact estimates across a continental shelf lagoon system. We explore how flooded extents and exposed population estimates from a 1% storm for Belize vary with estimated depths by comparing three existing bathymetries over a northern shallow, enclosed lagoon and a central deeper, open lagoon system with a newly developed bathymetry data set, Satellite-Derived Bathymetry Enhanced Data set-SDBED. We compare multiple bathymetric data sets to understand the influence on the flood uncertainties and the quantity of the impact of exposed population estimates. Our results show that greater estimated lagoon depths consistently result in lower predicted flood impacts for both lagoon systems in almost all cases. Unexpectedly, for one bathymetry with a median depth of 2 m in the northern lagoon, we find that a reduction in lagoon volume by 59% reduces total inundation volume by 45%. Our findings also show how vertical uncertainties in the SDBED bathymetry propagate through the model, resulting in variations of up to 12% in flood extents and up to 2% in exposed populations.

Plain Language Summary

The depth of the ocean floor close to the coastline is a critical input for models that predict flood extents during storms. Coastal flood models are especially sensitive to bathymetry data on shallow ocean features such as reef atolls and coastal lagoons. Data on shallow bathymetry are often difficult and expensive to obtain, and flood models typically rely on large-scale data sets that may not adequately describe important features such as lagoons or reefs. Despite the importance of shallow bathymetry, very little is understood about how differences in uncertainties, resolution, and descriptions of features within these data sets influence predictions of flood impacts. In this study, we compare four bathymetry data sets, including one developed in this study, and explore their influence on flood extent predictions within a coastal flood model for a reef-fronted lagoonal coastline in Belize in Central America. We find that variations between bathymetry data sets cause significant variations in predicted flood extents within shallow lagoons. Interestingly, our findings suggest that in a very shallow lagoon, inland flood extents are driven by the volume of water in the lagoon. We also find that uncertainties in these bathymetry data can cause variations in total area flooded by up to 12%.

1. Introduction

Coastal flooding due to tropical cyclones impacts hundreds of millions of people and billions of dollars of assets, and these global social and economic costs are expected to increase in the coming decades (Dullaart et al., 2021; Krichene et al., 2023). These projected flood damages are primarily driven by population growth and infrastructure development within exposed floodplains in the short term (Al-Attabi et al., 2023) and aggravated by climate change and sea-level rise over longer time periods (Barnard et al., 2019). The intensity of tropical cyclones has been increasing since 1980 and is projected to continue increasing with a warming climate (Knutson et al., 2020). Latin America and the Caribbean are among the most vulnerable regions globally to current and future tropical cyclone impacts, with over 2 million people and $178 billion (USD) in expected flood exposure by 2050 (Reguero et al., 2015).

Supervision: Zaid Al-Attabi, Siddharth Narayan, David Lagomasino
Validation: Zaid Al-Attabi, Anthony Campbell, Daystar Babanawo, Nathan Thomas, David Lagomasino
Visualization: Zaid Al-Attabi, Yicheng Xu
Writing – original draft: Zaid Al-Attabi
Writing – review & editing: Zaid Al-Attabi, Siddharth Narayan, Anthony Campbell, Ananth Wuppukondur, Daystar Babanawo, Nathan Thomas, Lola Fatoyinbo, David Lagomasino

The prediction of flood extents and damages from storm surges and waves during tropical cyclones relies on numerical models and multiple spatial data sets as inputs, of which bathymetry is a critical requirement (Al-Attabi et al., 2023; Dilmen et al., 2018; Menéndez et al., 2020). Variability in nearshore bathymetry and beach slopes can significantly alter the elevation and distribution of extreme water levels at the shoreline (Weaver & Slinn, 2010) and influence wave transformation processes (Serafin et al., 2019). Coastal structures and geomorphologic features such as atolls, barrier reefs, and lagoons also influence surge and wave transformation processes that impact the magnitude of wave height and reduce flooding onshore (Harris et al., 2018; Reguero et al., 2021).

Coastal lagoons are estimated to occupy 13% of the world's coastlines and up to 17% of the North American and Caribbean coastlines (Kennish & Paerl, 2010), but are poorly understood regarding their influence on storm surge compared to other coastal features. Coastal lagoons are shore-parallel water bodies that are separated from the ocean by a barrier such as a reef and are typically less than a few meters in median depth (Kjerfve, 1994). Found on all continents, including tropical coastlines such as the Caribbean, coastal lagoons are geologically relatively young geomorphological systems that have been studied in terms of their geology (Carrasco et al., 2016), ecology (Rodrigues-Filho et al., 2023), lagoon hydrodynamics (Lowe et al., 2010; McCabe et al., 2010), and circulation to assess human impacts such as pollution (Garces-Ordonez et al., 2022). Nearshore lagoon systems are also recognized as a challenge for satellite-derived and other remote-sensing bathymetric data collection approaches due to their turbidity, caused by suspended sediments reducing water clarity, which challenges optical satellite-derived bathymetry by limiting light penetration for optical remote-sensing bathymetry (Amrari et al., 2021). When they are enclosed, nearshore coastal lagoons, depending on their geometry, can either reduce or increase extreme water levels at the shoreline during storms (Lorenz et al., 2023). During a tropical cyclone, water levels in coastal lagoons are typically driven by tropical cyclone winds and tilting of the water surface (Kjerfve & Magill, 1989), with bathymetry becoming critical in determining water levels at the shoreline (Paugam et al., 2021). However, the effect of variations and uncertainty in bathymetry within lagoon systems on inland flood extents and impacts on population exposure are not well understood.

The Caribbean is home to the largest barrier reef system in the northern hemisphere, and this shoreline is among the most vulnerable to coastal flooding from storms and climate change, with more than 150 tropical cyclone impacts over the last 20 yrs (Jing et al., 2024; Martín et al., 2023). Belize contains over 25% of the Mesoamerican Barrier Reef system (Gress et al., 2019). This reef system creates a highly complex nearshore zone, characterized by a narrow continental shelf but bordered by extensive reefs. This creates a large nearshore lagoon (>4,300 km^2), separating the barrier reef system from the mainland (Figure 1a). The Belize continental shelf lagoon system is divided into five regions based on bathymetry, with depths increasing from the shallow north, with a median depth less than 3 m, to the deeper south with a median depth greater than 60 m: Chetumal Bay, the northern shelf lagoon, the central shelf lagoon, the southern shelf lagoon, and the Gulf of Honduras (McNeill et al., 2010). The northern shelf lagoon extends from the northern border of Belize south to Belize City, the largest and most populous city in Belize, while the central shelf lagoon stretches from the southern tip of Belize City to the south (Figure 1a). During a storm, lagoon bathymetry can greatly influence storm surge impacts on such a coastline. However, high spatial resolution nearshore bathymetry is often unavailable in tropical coastlines, or when available, does not include key nearshore features such as lagoon systems due to issues related to access and cost (Hsiao et al., 2016). The reliance of numerical models on bathymetry data with limited spatial detail on nearshore features, especially on reef and lagoon-lined coastlines, has been previously shown to reduce the accuracy of flood damage estimates by up to a factor of 1.25 (Parodi et al., 2020). Despite recent advances in ocean bathymetry related to initiatives such as the Seabed 2030 Initiative (Mayer et al., 2018) and the Allen Coral Atlas (ACA) (Lyons et al., 2024), coverage of the nearshore region remains limited to the immediate vicinity of coral reefs and continues to face inherent limitations, particularly in shallow turbid waters and sharp nearshore slopes (Gou et al., 2023; Weaver & Slinn, 2010).

Here, we explore how variations in bathymetry of shallow nearshore regions influence estimated total inundation volumes, peak flood and wave heights, and exposed population for the lagoon-fronted coastline of Belize. We develop a high-resolution bathymetric data set, hereafter called Satellite Derived Bathymetry Elevation Data set (SDBED), covering the nearshore region of Belize and quantify how variations in nearshore bathymetry influence predicted storm surge impacts from a 1% storm. The SDBED is developed by integrating a satellite-derived bathymetry data set for clear shallow waters using ICESat-2 and Landsat imagery with data from nautical charts for the turbid lagoon and previously published reef profile measurements (Kobara & Heyman, 2010) to capture sharp slopes in the fore-reef zones. Using a 2-D hydrodynamic model, we predict the number of people flooded from a 1% storm modeled after Hurricane Hattie in 1961, the strongest storm on record to make landfall in

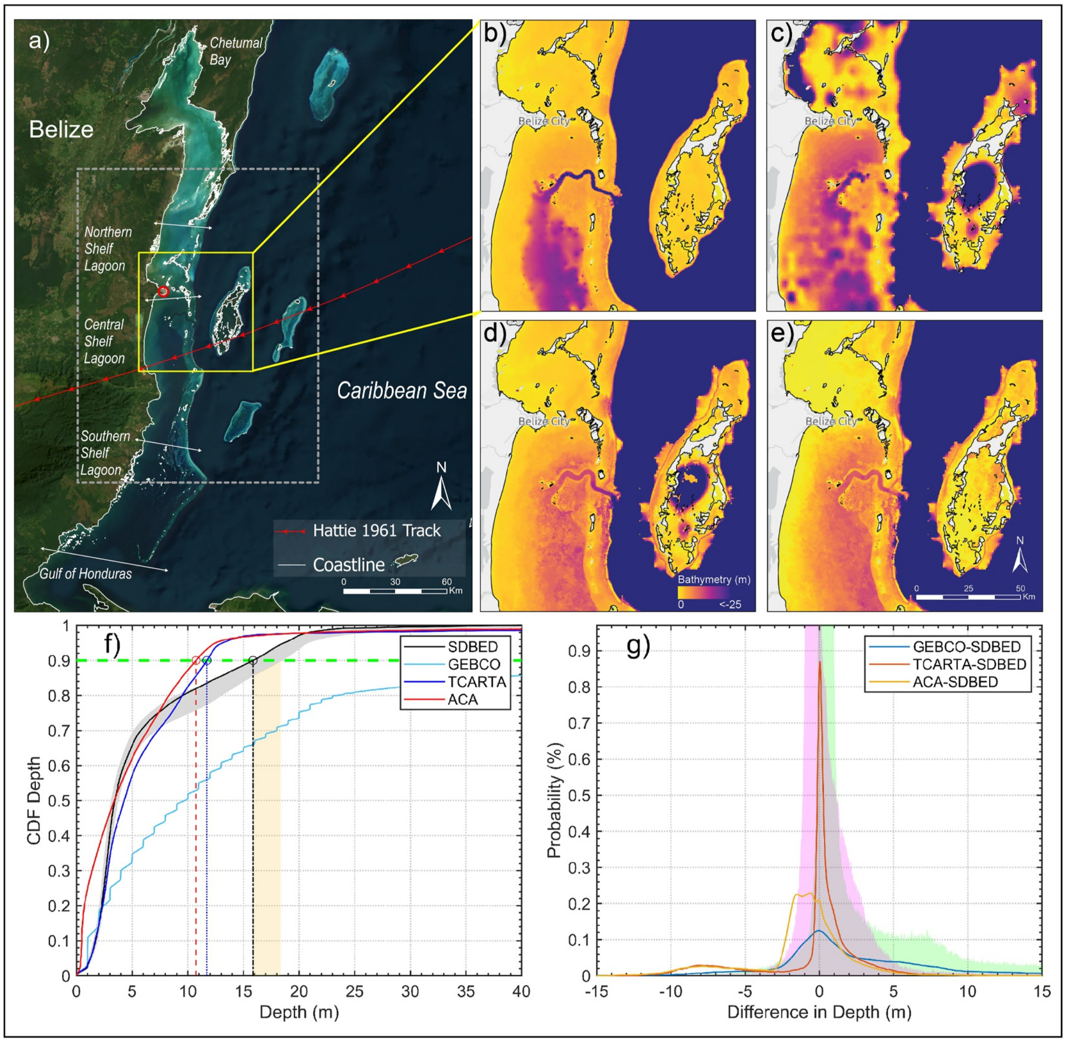

Figure 1. Bathymetric models show differences in water depth that vary with location and geomorphology. Panel (a) shows a satellite image of the Belize continental shelf lagoon system, highlighting the coastline (white line), the path of Hurricane Hattie 1961 (red arrow line); the red circle shows Belize city; the gray dashed box shows the area of the model with 100 m spatial resolution; and the yellow box shows the center of the model domain, highlighting different near/offshore features such as the northern shelf lagoon and central shelf lagoon, reef barriers, and atoll. Horizontal white lines denote approximate lagoon bounds. Panels (b) through (e) show bathymetric maps of Central Belize based on different bathymetry data sets: (b) SDBED, (c) GEBCO, (d) TCarta, and (e) ACA data sets. Panels (f, g) present cumulative distribution functions (CDFs) and probability distributions of estimated depth for the four bathymetry data sets, respectively. In panel (f), the gray-shaded area represents the standard error of the SDBED data sets, and the green and pink shading in panel (g) refers to the probability distributions for SDBED+ and SDBED- relative to SDBED. The horizontal green line in panel (f) indicates a 90% cumulative probability, vertical lines show the corresponding x-axis values for each data set, and the yellow-shaded area reflects the 90% cumulative probability range within the SDBED standard error. Data are binned by 0.01 m.

Belize (Dunn, 1962). We compare the spatial distribution of flooded extents and population exposure between SDBED and three other bathymetry data sets available for Belize, namely, the Allen Coral Atlas (hereafter, ACA), the TCarta Satellite-Derived Bathymetry, and the General Bathymetric Chart of the Oceans-GEBCO. We also investigate how vertical uncertainties in the SDBED data set and variations in population data influence predicted flood impacts, flooded extent, and exposed population. We show that predicted flood impacts are particularly sensitive to variations in nearshore bathymetry within the shallow, enclosed northern shelf lagoon, whereas in the deeper, more open central lagoon, greater lagoon depths are consistently associated with lower flood impacts across all data sets. We also show that while higher-resolution population data sets (e.g., WorldPop at 100 m) reduce variability in exposure estimates across bathymetries, differences remain substantial (up to 40,000 people), underscoring the importance of accurate bathymetry models for vulnerable coastal regions.

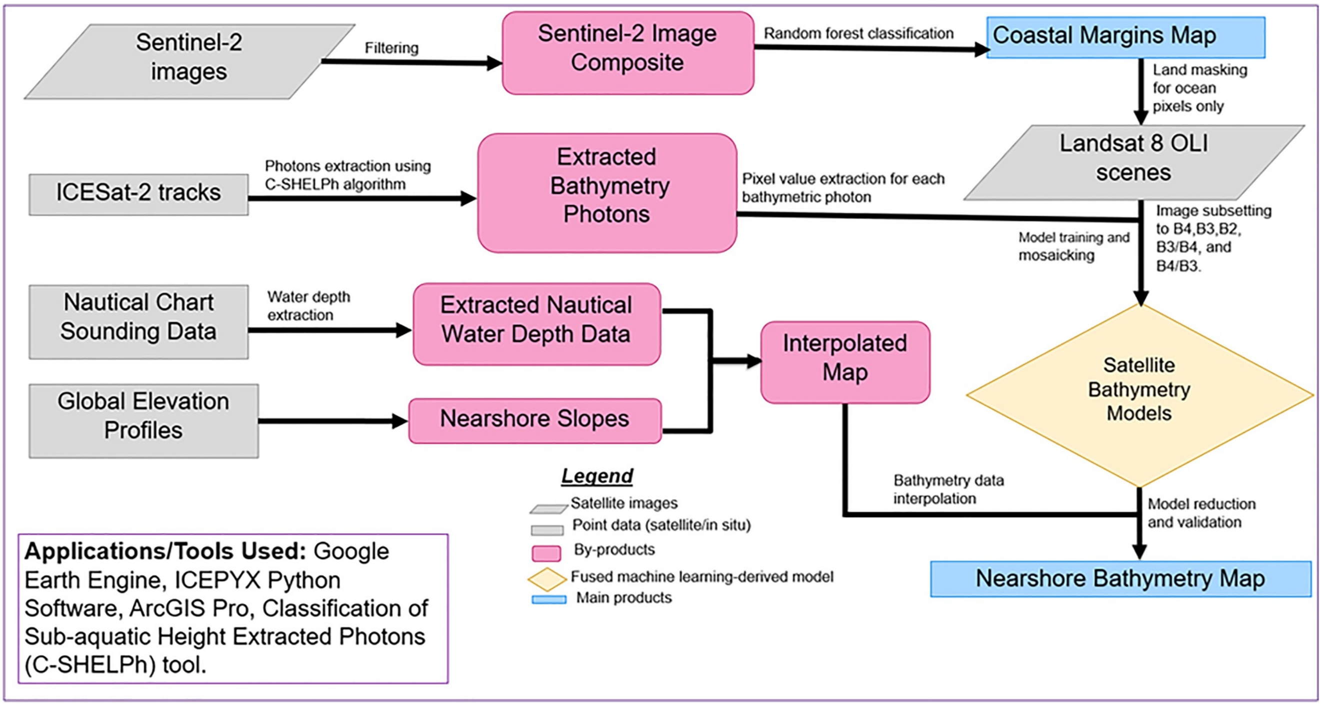

Figure 2. The flowchart summarizes the methodology followed to derive the SDBED data set.

2. Materials and Methods

2.1. Satellite-Derived Bathymetry (SDBED) for the Nearshore Regions of Belize

We developed a nautical- and slope- augmented Satellite-Derived Bathymetry data set (SDBED) up to the 200 m depth contour for the Belize nearshore region that combines information from nautical charts, satellite-derived bathymetry, field-based slope contours, and GEBCO data. As a first step, we delineated the coastal margins of Belize into four distinct groups based on spectral characteristics: Land, Shallow Water, Intermediate Water, and Deep Water. To generate this layer, we created a 20th-percentile composite of Sentinel-2 images acquired between June 2020 and June 2023, which reduces the influence of clouds and transient turbidity (Traganos et al., 2018). We then applied a Random Forest (RF) classification model trained to the four separate categories based on visual interpretation of the Sentinel-2 20th percentile composite. The coastal zone classification output defines where ICESat-2 bathymetric photons can be reliably collected and identifies regions where optical satellite-derived bathymetry is limited by turbidity and depth. This coastal margin layer provides the spatial mask for integrated satellite-derived bathymetry within the shallow and intermediate classes but nautical charts or GEBCO within the deep-water class (Figure 2).

We accessed ICESat-2 data for the study regions from the National Snow and Ice Data Center (NSIDC) using the icepyx Python software (The icepyx Developers, 2023). We categorized bathymetric photons using C-SHELPh, a Python algorithm developed by Thomas et al. (2022) to efficiently extract bathymetric photons from noise. Following the automated processing, we perform a final visual inspection of the data to remove erroneous points such as shallow returns in deep water from wave troughs or noise from the water column. In Belize, we observe that ICESat-2 can penetrate to a maximum depth of ~23 m due to water quality and turbidity, which can scatter and absorb the laser light, reducing the effectiveness of the sensor in capturing accurate bathymetric measurements.

We acquired Landsat 8 OLI atmospherically corrected surface reflectance (Collection 2/Tier 1) scenes (over a 1-year period (2022-01-01 to 2022-12-01) for the study region via the Google Earth Engine (GEE) catalog and preprocessed these data for satellite-derived bathymetry modeling. For these analyses, we focused on the visible spectrum bands, including the blue (SR_B2), green (SR_B3), and red (SR_B4), and a calculated ratio of blue/green bands. Each image was pre-processed to remove clouds and cloud shadows using standard cloud masking procedures (Coluzzi et al., 2018). These spectral variables were then paired with the ICESat-2 bathymetric photon depths to train Random Forest (RF) regression models, enabling the statistical relationship between water surface reflectance and seafloor depth. The ICESat-2 water depth data were randomly split into training and validation data for training and test model performance. We applied two separate training/validations in order to have an equitable distribution of points across shallow and intermediate water depths, as a large majority of points fall within the shallow water zone. For the ICESat-2 water depth classified photons that intersected with the shallow coastal zone, we randomly selected 5% for training and 95% for validation following similar procedures in Thomas et al., 2022, but we did not ground-truth the predicted depths with sonar data. As a modification and to ensure model training with deeper water depths, ICESat-2 data that intersected with the intermediate water depth class were split into 70% for training and 30% for validation. Despite observed water depth values of ∼23 m, this process of random sampling and masking to the shallow and intermediate water zones resulted in water depth training data from ICESat-2 that was between 0.7 and ∼15.7 m. The training data were then combined with the corresponding pixel-wise Landsat 8 spectral data for each available cloud-masked image over the 1-year period, resulting in multiple water depth maps, one for each available Landsat eight image with valid pixels over the coastal zones. Finally, we reduce the collection of water depth maps to a single 2022 bathymetry map using descriptive statistics (mean, median, and standard deviation) as follows (Thomas et al., 2022). The reduction to a single composite allows for the generation of a robust bathymetric model with high accuracy and low root mean square error (RMSE) values. It also enables the spatial distribution of uncertainty to be mapped across the study region at high resolution (Thomas et al., 2022).

We used publicly available nautical chart data (www.gpsnauticalcharts.com/) within the 0–200 m contour to fill in gaps in the bathymetry that occur outside the shallow and intermediate coastal zones used in the Satellite-Derived Bathymetry. Using the nautical charts, we hand-digitized sounding measurements across the lagoon and tidal channels. These individual points were imported into ArcGIS Pro and used in a surface contour map to create an interpolated seafloor map. For additional gaps along the reef edges, we used slope profiles for Turneffe Atoll and Lighthouse Reef from Kobara & Heyman, (2010), who conducted field measurements of profile elevations along multiple reef edges of the central Belize shoreline. We used the median profile for each reef atoll and linearly extended it up to 200 m. Beyond the 200 m depth contour, we merged our data set with GEBCO. The SDBED, nautical chart, profile, and offshore GEBCO data sets were merged into a seamless bathymetry data set in ArcGIS Pro. In short, SDBED integrates ICESat-2-calibrated Landsat-derived depths (0–15.7 m) with nautical charts (turbid and deeper areas) and reef profiles (sharp slopes), merged seamlessly win ArcGIS Pro using kriging interpolation at the 0 m contour. Topography from corrected SRTM (90 m resolution, vegetation bias removed; original SRTM is 30 m resolution) was blended with bathymetry at the coastline using bilinear interpolation to ensure continuity.

2.2. Evaluation of Vertical Uncertainties and Comparisons With Other Data Sets

To evaluate the effect of vertical uncertainties in SDBED, we calculated the standard error for each pixel of SDBED and created two additional data sets representing bathymetry values deeper by one standard error (SDBED+) and shallower by one standard error (SDBED-) for each pixel. We estimated these uncertainties for two components of the data set: the satellite-derived bathymetry and the reef profile data. To estimate uncertainty in the reef profiles, we calculated the mean and standard deviation across all reef slopes. We compare the distribution of depths from SDBED (30 m original resolution) with two other high-resolution satellite-derived bathymetry data sets–TCarta (90 m) and Allen Coral Atlas (ACA) (10 m) and one coarse, 460 m resolution bathymetry data set–GEBCO (Tables S1, S2 in Supporting Information S1). All data gaps in the TCarta and ACA data sets were filled with data from GEBCO. All bathymetry data sets were resampled to the model's 100 m grid; even post-resampling, higher original resolutions enhance nearshore feature representation, influencing flood outcomes. While resampled to 100 m, higher original resolutions in SDBED/TCarta/ACA yield more accurate feature representation than coarser GEBCO, highlighting the value of high-resolution inputs despite model grid constraints.

To explore the effect of spatial resolution on nearshore feature descriptions across data sets, we upsampled the 100 m SDBED to 460 m using cubic convolution and visually compared this data set with the original 100 m SDBED and the upsampled 460 m SDBED to GEBCO data sets.

2.3. Modeling Wave Heights, Flood Extents, and Number of People Flooded

We used a two-way coupled flow and wave model, 2D Delft3D FM Flow and SWAN models, to simulate present-day (2021) flooding from a ∼1% storm in Belize (Figure S1, Text S1, S2 in Supporting Information S1) for multiple bathymetry and population data set scenarios. The selection of the 1% storm was carried out first by empirically estimating annual exceedance probabilities by sorting and ranking the maximum wind speeds of 46 historical storms between 1940 and 2023 that passed within a 100 km radius of the Belize coastline (Figures S2, S3 in Supporting Information S1). We fitted a polynomial regression model on these events and on this basis selected Hurricane Hattie, which made landfall in 1961. Hurricane Hattie caused $60 million in damages in 1961 USD, or $630 million in 2025 USD, and more than 262 deaths (Dunn, 1962).

For the flow module, we generated an unstructured nested grid of varying resolutions (6.4 km in the offshore regions to 100 m in the nearshore region around central Belize and covers up the atoll offshore) from the outer Caribbean Sea into the coastal floodplain around Belize up to a topographical elevation of 10 m above mean sea level. The high-resolution, that is 100 m, floodplain considered in the analysis is 1,322 km^2, comprising a 178 km stretch along the Belize coastline, extending 74 km north and 104 km south of Belize City and up to 94 km offshore, covering the Turneffe Atoll and Lighthouse reefs. For the rest of Belize, outside our region of interest, the model utilizes a variable spatial resolution ranging from 100 m to 1.5 km (Figure S1 in Supporting Information S1). The hydrodynamic model includes the effect of waves when computing total water levels. Wave contributions to total water levels in each wet grid cell were computed by coupling the Delft3D flow model to the SWAN wave model. The coupled model implicitly incorporates wave setup through radiation stress gradients but does not compute setup or runup as explicit parameters.

Along the open boundaries of the flow module, we obtained tidal forcing conditions from the TPXO 8 global tide model (Egbert & Erofeeva, 2002), as discussed in Supplementary Section 3. We used spatial (0.5-degree resolution) and time-varying (at every 6 hr) wind vector and atmospheric pressure data sets from ERA5 ECMWF reanalysis as external force inputs for simulating the tropical cyclone between the dates 1961/10/24 and 1961/11/1 (Hersbach et al., 2020). We used global land cover data published by the European Space Agency in 2021 to define the Manning's n friction coefficients within the domain (Zanaga et al., 2022), using class values provided by Zhang et al. (2012) (Table S3 in Supporting Information S1). For the DEM, we used a modified version of the global Shuttle Radar Topography Mission-SRTM 30 m data set, corrected for coastal elevations in Belize, to account for errors due to the incomplete removal of tree cover elevations at the coastline (Sampson et al., 2016). Systematically removing vegetation bias using satellite-derived data results in improving the vertical accuracy of SRTM by reducing the error from 15.8 m to just 0.1 m (Sampson et al., 2016).

First, we validated the model with just the tidal signal (without tropical cyclone forcing) to calibrate the numerical parameters such as mesh resolution, calculation time step, and friction factors (Figure S4, Table S4 in Supporting Information S1). We then set up and calibrated the model, particularly the wind drag coefficients for Hurricane Michael 2018 with cyclonic wind forcing (values of 0.0025 and 0.05 for 0 m s-1 and 100 m s-1 wind speeds, respectively). We validated the coupled storm surge and wave model for wave heights and total water levels during Hurricane Michael 2018 in Belize, and the model shows very good performance against measured heights with RMSE values <0.06 m, <15% for water levels, and <0.22 m, <11% for wave heights (Figures S5, S6, and Tables S5–S8 in Supporting Information S1). The model was validated against Hurricane Michael (2018) due to available water level and wave observations. Later, we set up the coupled model for Hurricane Hattie 1961 and once again validated the computed total water levels against the only available field observation of a high-water mark (∼3.8 m) recorded near the Belize city shoreline for that event (Dunn, 1962; Nancoo, 1962). The model shows a good agreement against the high-water mark with an RMSE of 0.11 m. Peak flood heights are calculated as the depth of water above dry land. All bathymetry, land elevations, total water level, and flood heights are referenced to the mean sea level (MSL) vertical datum for Belize.

3. Calculating Lagoon Volumes and Flooded Populations

We used the four bathymetry data sets as inputs into a coupled storm surge-wave hydrodynamic model, Delft3D FM FLOW and SWAN models (Booij et al., 1999; Holthuijsen, 2010; Ris et al., 1999) with a maximum grid resolution of 100 m, and calculated for each of these bathymetry data sets the flood extents and total inundation volume for a 1% storm modeled after Hurricane Hattie, which made landfall in central Belize in 1961 (Figure S7 in Supporting Information S1). All bathymetry data sets were resampled to the model grid resolution. To estimate bathymetry effects on lagoon volume, we calculated the volume of water below MSL (excluding tidal variations) by integrating bathymetric depths over the defined lagoon area in each bathymetry data set for the two lagoons.

To understand the importance of differences in bathymetry products against other model inputs, that is, population exposure, we compared model results in terms of total people flooded using 3 publicly available population data sets for the region: WorldPop with a resolution of 100 m (Bondarenko et al., 2020), the Gridded Population of the World (GPW) with a resolution of 1000 m (Warszawski et al., 2017), and Global Gridded Population (GlobPOP) with a resolution of 1000 m (Liu et al., 2024) across all bathymetric inputs (Table S9 in Supporting Information S1). For the 12 combinations of population and bathymetry data sets, we counted the total number of people inside all areas where peak flood heights were greater than 0.1 m. The number of people impacted by flooding was calculated by overlaying the flood extent with the population grid using the Tabulate Intersection tool in ArcGIS Pro; if the flood covered more than 50% of a population cell, the entire population of that cell was counted to provide an upper-bound exposure estimate.

4. Results

4.1. Comparison of New Satellite-Derived Bathymetry With Existing Data Sets

We developed a new bathymetric product, SDBED, that provides 30 m horizontal resolution data on seafloor depths down to 200 m for Belize, capturing the nearshore lagoon complex, inlets, and reef slopes, as well as the barrier and atoll reefs and their lagoons (Figure 1b). A visual comparison to high-resolution satellite imagery shows that SDBED captures nearshore geomorphic features not present in GEBCO (Figures 1b and 1c) and shows slight differences to TCarta and ACA, especially within the nearshore shelf lagoon and around the atolls (Figure S8 in Supporting Information S1). For example, the inlet channel in the central lagoon is nearly absent in GEBCO (Figure 1c) but is distinct in SDBED, ACA, and TCarta (Figures 1b–1d and 1e). However, SDBED results in water depths up to 9 m deeper in the central lagoon and channel (see Figures 1b–1d and 1e) compared to ACA and TCarta. The SDBED also provides more detail compared to all other data sets on the sharp reef slopes outside the lagoon's barrier reef and around the atolls and is overall more comparable to TCarta than to GEBCO and ACA (Figures 1d–1f).

Median vertical uncertainty in the SDBED data sets is less than ±0.28 m. However, within the northern shelf lagoon, where most of the predicted flooding occurred, the median uncertainty is ±0.15 m, which is within the tidal range for the lagoon. Probability distributions of vertical uncertainty in SDBED show that >96% of the data set has an uncertainty of less than 0.5 m (Figure 1g). Moreover, SDBED also exhibits differences in the probability distributions of depth compared to the other three data sets, tending to be deeper than ACA but slightly shallower than TCarta (Figure 1g). In the northern shelf lagoon, depth values for SDBED depths are significantly different from ACA and GEBCO but indistinguishable from TCarta (Figures 3a and 3b) (Table S10 in Supporting Information S1).

4.2. Differences in Predicted Flood Extents and Peak Flood Heights Across Bathymetries

There is high variability between the four bathymetry data sets in terms of where flooding happens, but the majority of onshore flooding occurs adjacent to the northern shelf lagoon, a shallow, well-enclosed basin (Figures 3h and 3i; Table S10 in Supporting Information S1). Flood extents based on SDBED and TCarta are nearly identical, covering an area of 1,126 and 1,127 km^2, respectively, whereas the ACA-based model resulted in a 6.5% lower flood extent of 1,052 km^2. A reduction in flood extent of 20% was found with the GEBCO model, which flooded 896 km^2. GEBCO and ACA both predict lower peak flood heights compared to SDBED, with the 90% CDF of peak flood heights reaching 1.6 m for GEBCO and <1 m for ACA, versus 2.4 m for SDBED (Figure 4c). Peak flood heights predicted with TCarta are in good agreement with SDBED, with minor variations up to ±0.2 m with a small probability of 2% (Figure 4d).

Uncertainties in SDBED bathymetry affect flood simulations, with the SDBED- data set being shallower by one standard error per pixel, leading to higher peak flood heights, up to 0.83 m compared to the original SDBED data set. The deeper SDBED+ results in lower peak flood heights, up to 0.62 m lower compared to the SDBED data set (Figure S9 in Supporting Information S1). The shallower SDBED- model thus predicts a slightly larger flooded area of 19 km^2 or ~2% compared to SDBED. Conversely, the deeper SDBED+ results in a lower storm surge and

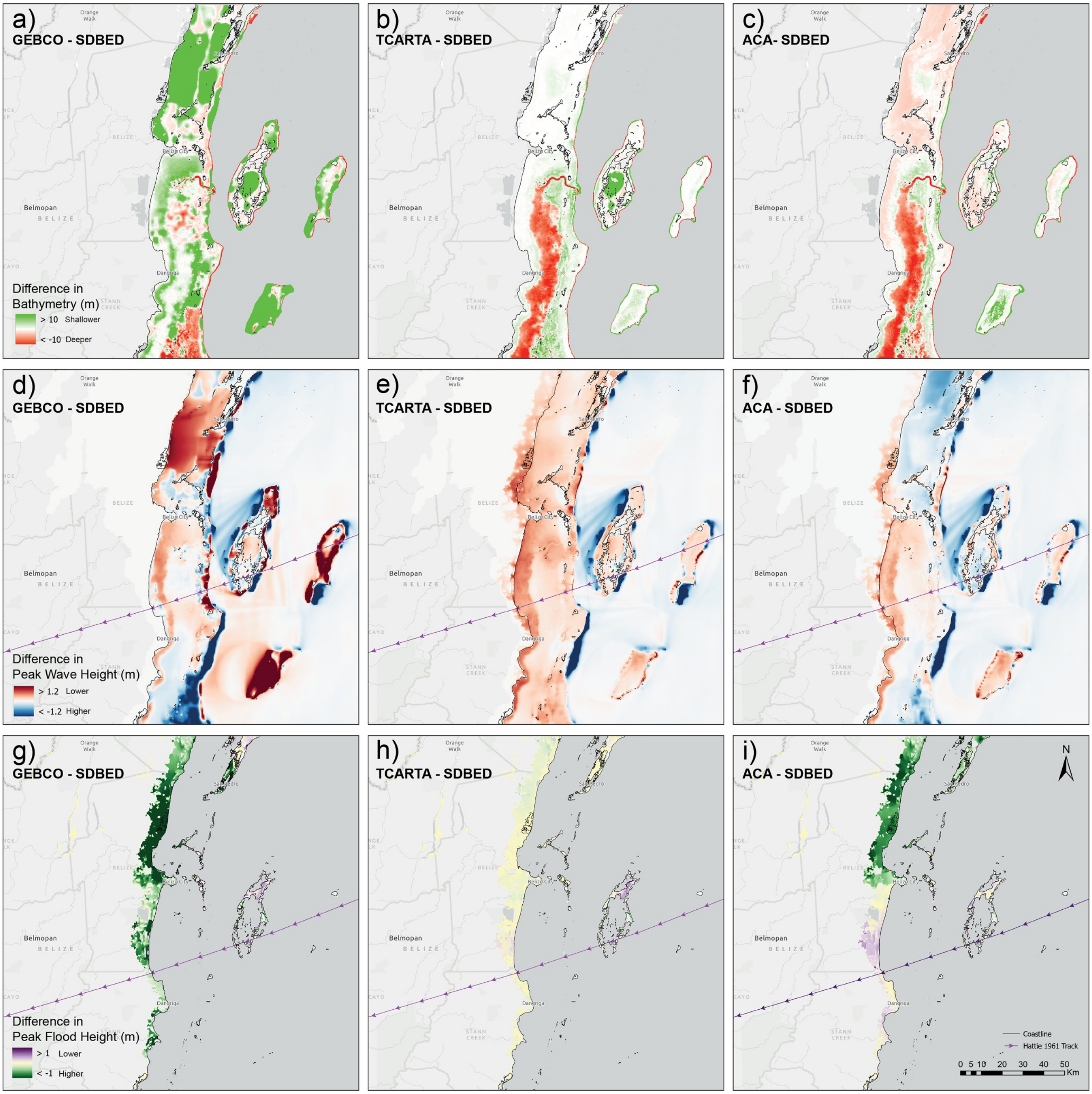

Figure 3. Small differences in water depth between bathymetry models influence wave and peak flood heights for shallow lagoons. Maps showing spatial differences between GEBCO–SDBED (left), TCarta–SDBED (middle), and ACA–SDBED (right) for estimated depths (top row, panels a–c), peak wave heights (middle row, panels d–f), and peak flood heights (bottom row, panels g–i). All depths >40 m are shown in gray. The terms "Higher," "Lower," "Shallower," and "Deeper" in the map scale indicate the overestimations and underestimates of SDBED relative to the other three data sets.

a reduced flooded area of 116.8 km^2 or ∼10% compared to SDBED. The probability of differences shows that the deeper SDBED+ has a higher probability of underpredicting peak flood heights compared to the shallower SDBED (Figures 4c and 4d).

We found that lagoon volume is an important controlling factor for determining overall inundation on land (Figure 5). Lagoon volume is estimated as the volume below MSL (excluding tidal variations), calculated by integrating bathymetric depths over the defined lagoon area in each bathymetry data set. In the deeper central shelf lagoon, we found consistent relationships between lagoon volume and inundation volume across all

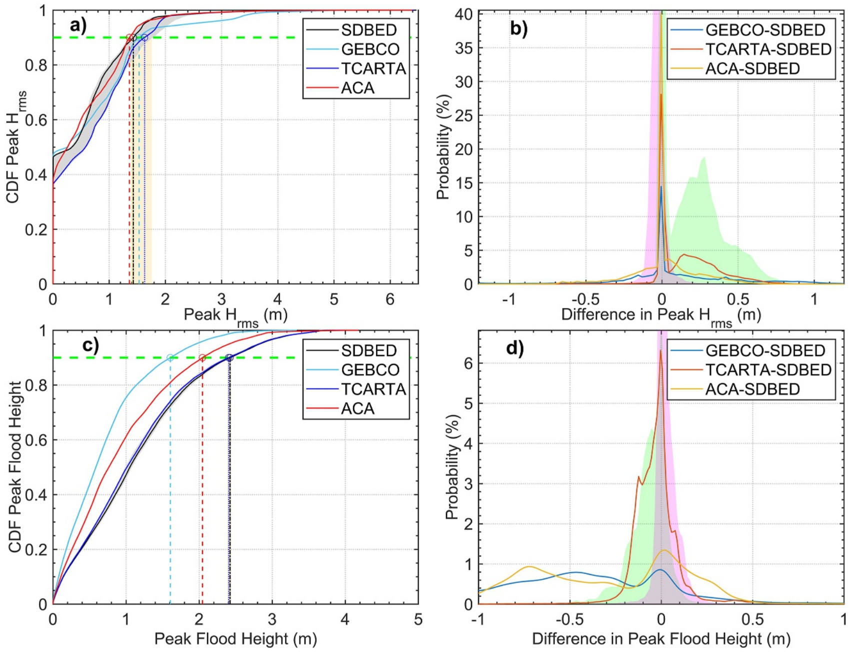

Figure 4. Using different bathymetry models has relatively small influence on wave height but alters peak flood outcomes. Cumulative distribution functions (CDFs) (left; panels (a–c)) and probability distributions (right; panels (b, d)) of predicted peak wave height (Hrms) (top row) and peak flood height (bottom row) for the four bathymetry data sets. The gray-shaded areas represent the standard error of Hrms and peak flood height from the SDBED scenario. The yellow-shaded area represents the 90% cumulative probability range for the standard error SDBED estimates. Data are binned by 0.01 m. Green and pink shaded areas denote the probability distributions of differences between SDBED+, SDBED-, and SDBED estimates. Horizontal green lines in panels (a, c) indicate a 90% cumulative probability, with vertical lines showing the corresponding *x*-axis values for each bathymetry data set.

bathymetry data sets (Figures 5a–5e). Here, an increase in lagoon volume is correlated with a decrease in inundation volume and vice versa. An increase in lagoon volume of 12% with GEBCO, compared to SDBED, results in a decrease in onshore inundation volume by 61%. A decrease in lagoon volume of 15% with ACA, compared to SDBED, results in an increase in inundation volume by 12% (Figures 5c and 5d). A two-sample KS test in the central shelf lagoon found significant differences between SDBED compared to GEBCO and ACA but no significant differences in estimated volumes between SDBED, TCarta, and the standard error SDBED- and SDBED+ data sets (Figures S10, S11 in Supporting Information S1).

In the shallower and more enclosed northern shelf lagoon (Figures 5f–5j), the relationships between lagoon volume and total inundation are also consistent across bathymetry data sets, except for the ACA data set, where median lagoon depth is less than 2 m. The shallower depths estimated in ACA result in a 59% lower lagoon volume and a 45% lower total inundation volume (Figure 5j). The GEBCO model estimates much larger lagoon depths, resulting in a lagoon volume ~250% greater than SDBED, but in contrast to ACA, these greater depths result in a 56% decrease in total inundation volume (Figures 5h–5j) (Table S10 in Supporting Information S1). Here again, two-sample KS tests in the northern shelf lagoon found significant differences between SDBED compared to GEBCO and ACA but no significant differences between SDBED, TCarta, SDBED-, and SDBED+ (Figures S12, S13 in Supporting Information S1).

4.3. Differences in Predicted Peak Wave Heights Across Bathymetries

Variations in nearshore depths also influence peak wave heights during the storm, with greater water depth resulting in higher predicted peak wave heights. The 90% probability maximum wave height values ranged from 1.3 to 1.6 m for all four data sets (Figure 4a). The deeper GEBCO bathymetry resulted in a greater proportion of wave heights over 2 m (6%) compared to between 2% and 2.6% for SDBED, ACA, and TCarta. Overall, SDBED compares better to ACA and TCarta than to GEBCO, with the probability distribution of wave height differences showing that only 10% of wave heights predicted by GEBCO match those predicted by SDBED, compared to 28%

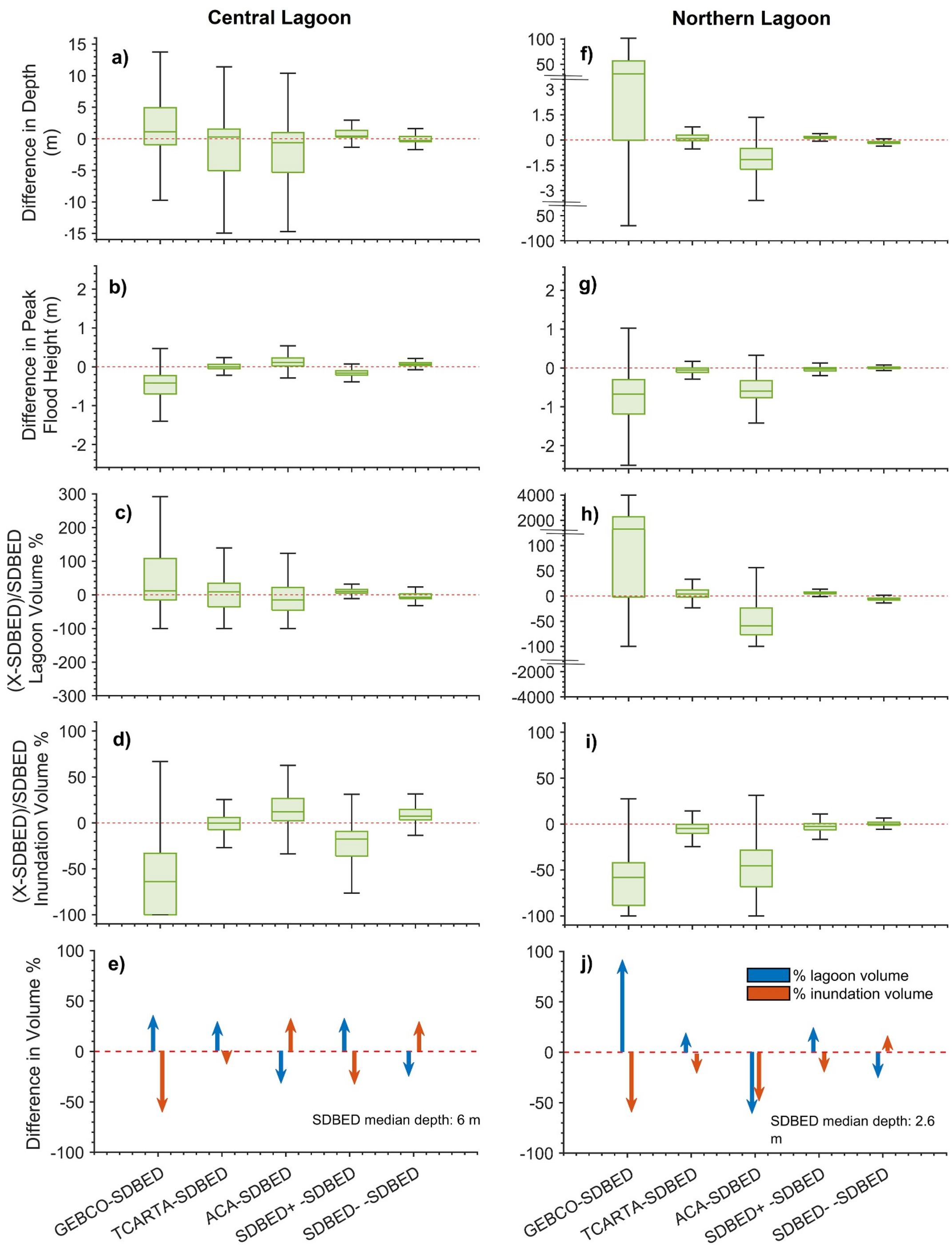

Figure 5. Differences in lagoon volumes have contrasting relationships with total inundation based on geomorphology for the central lagoon (left) and northern lagoon (right). Panels (a, f) show the difference in the bathymetries; Panels (b, g) refer to the differences in the peak flood height in m; Panels (c, h) show the percentage of difference in the lagoon volumes; Panels (d, i) refer to the percentage of difference in the inundation volumes; Panels (e, j) refer to the diagram of difference in the inundation and lagoon volumes.

for TCarta and 40% for ACA (see Figure 4b). Vertical uncertainties in the SDBED bathymetry data set influence predicted peak wave heights, with a bias toward higher wave heights. The majority of wave heights estimated with the shallower SDBED- data set are up to 0.1 m lower than the median data set, while 5% of the deeper SDBED+ estimates are higher than the median by 0.3 m (Figure 4b).

Spatially, wave heights calculated using SDBED differed most from the other data sets around the edges of the reefs and reef atolls and inside the northern shelf lagoon (Figures 3d–3f). Around the edges of the reefs and reef atolls, SDBED predicts higher wave heights compared with all other data sets. The largest differences between SDBED and GEBCO are inside the offshore atolls and within the northern and central shelf lagoons. SDBED produces peak wave height values that are up to 4 m lower than GEBCO in the northern shelf lagoon and up to 5 m higher in the central shelf lagoon (Figure 3d). Peak wave heights with SDBED are lower than TCarta values within the entire lagoon (Figure 3e), whereas they are higher than ACA in the northern shelf lagoon (Figure 3f).

4.4. Population Flooded

The higher resolution bathymetries, TCarta, SDBED, and ACA, with a data resolution of 100 m or finer, that are interpolated within the model to the grid resolution of 100 m, result in exposed population estimates ranging from ∼49,000 to ∼93,000 people across all population data sets. However, the GEBCO data set with spatial resolution of ∼460 m resolution, resampled within the model to 100 m grid resolution, results in exposed population estimates ranging from ∼37,000 to ∼52,000 across all population data sets (Table S11 in Supporting Information S1). The differences in the predicted number of people flooded are largest between TCarta and GEBCO for all population data sets, ranging from ∼13,000 to ∼41,400 fewer people flooded for GEBCO (Figure 6). Aligning with our results of inundation area, SDBED and TCarta had similar exposed populations across their respective population data sets. This is largely a result of similar spatial flooding extents around Belize City (Figure 6). The ACA-based flood models were consistently lower than SDBED and TCarta across all three population data sets but greater than the GEBCO models. This is in line with the predicted flood extent of ACA (Figure 6) being lower than that of SDBED and TCarta in Belize City (Figure 6). Vertical uncertainties in the SDBED data set propagated through the flood models and showed a difference of ∼1400–2100 people depending on the population data set used.

Across population data sets, GPW 2020 shows the lowest number of people affected by flooding, whereas GlobPOP 2020 consistently shows the highest number of people affected. The GlobPOP 2020 data set had the highest variation in exposed population estimates across all four bathymetries of 41,400 people compared to WorldPop 2020, with 26,400 people (Figure 6, and Table S11 in Supporting Information S1).

5. Discussion and Conclusions

This study explores how differences in nearshore bathymetry influence model estimates of coastal flooded extents and populations. Using four bathymetry data sets, SDBED, TCarta, ACA, and GEBCO, our study describes how uncertainties and variability in bathymetry translate to estimates of flooded areas and people. This study does not address the accuracy or quality of the depth estimates from the new SDBED relative to other bathymetry data sets but rather shows through multiple comparisons that spatial and vertical variations in nearshore bathymetry can have a strong influence on predicted flood extents and thus population exposure estimates. Our findings also show that differences in coastal lagoon morphologies (i.e., shallow vs. deep) play an important role in the volume of water that can be transported onshore during storms.

This study shows that predicted flood impacts are sensitive to changes in estimated depth in the order of 1–2 m in a shallow lagoon. In both lagoon systems in our study, inundation volumes and impacts on land are inversely related to lagoon depths, as shown by previous studies (Parodi et al., 2020) across all but one bathymetry data set. We find the opposite for the shallowest bathymetry in the northern lagoon, where a reduction in depth results in lower inundation extents on land. Although this has not been studied for lagoon systems, similar models for coral reefs find that flood impacts are sensitive to changes in reef crest bathymetry of 0.1–1 m (Beck et al., 2018). While flooding across lagoon morphologies has not been explored extensively, previous research suggests that in shallow, enclosed lagoons, consistent, directional winds, such as during storms, can cause a tilting of the water surface, a process highly dependent on lagoon depths (Paugam et al., 2021). In contrast to the central shelf lagoon, total inundation volumes across the relatively shallow and enclosed northern lagoon are highly variable between SDBED, GEBCO, and ACA, with a difference of 1.16 m in median depth between SDBED (2.6 m median depth) and ACA, resulting in a 45% difference in total inundation volume. This suggests that bathymetric uncertainty is a major component of flood extent variability in shallow lagoons with median depths <2 m. Our results are influenced by Hattie's specific track. Flood variability in the northern lagoon is enhanced by onshore winds in Hattie's right-front quadrant, while similarities in the southern lagoon may not hold for alternative tracks, for

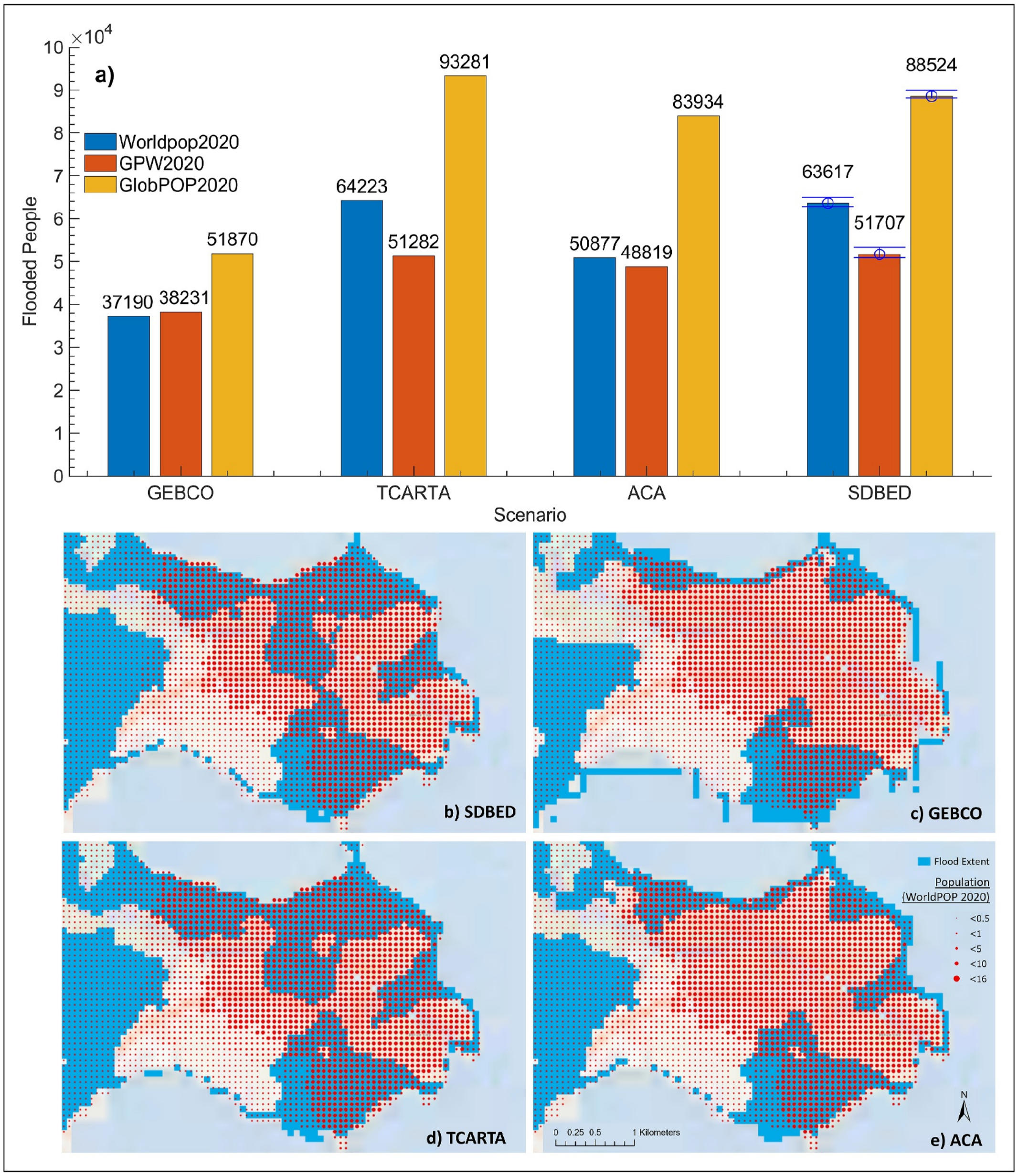

Figure 6. The estimated number of people flooded varies across data sets but is influenced by small changes in bathymetry. Panel (a) highlights the number of people flooded >0.1 m for each of the four bathymetry data sets and each of the three population data sets: WorldPop 2020 (blue), GPW 2020 (red), and GlobPOP 2020 (yellow). Blue lines for SDBED represent the population estimates for ± standard error data sets as labeled, and the circles represent the median SDBED estimates. Spatial WorldPop 2020 population density (red circles) and the peak flood extent (blue-shaded region) in Belize city predicted based on different bathymetry data sets: (b) SDBED, (c) GEBCO, (d) TCarta, and (e) ACA data sets.

instance, southward approaches. While our model simulations demonstrate sensitivities to bathymetry for the same hurricane characteristics, it is possible that these sensitivities are different for different hurricane tracks. Our use of Hattie's wind speeds as a 1% event is also event-based and may not yield the true 100-year surge, which requires response-based probabilistic modeling of multiple storms. Future work could extend this to synthetic storm ensembles to better represent return periods and isolate bathymetric influences.

Accurate resolution of bathymetry in lagoon morphologies is challenging but important for understanding storm surge impacts. Our study suggests that ICESat-2-based satellite-derived bathymetry is suitable for the task. Lagoon-fronted coastlines are found throughout the Caribbean (Beddows et al., 2016; Carrasquilla-Henao et al., 2022; Gonzalez-De Zayas et al., 2021). Field measurements of bathymetry can be challenging given navigational obstacles and the high cost of the platforms. We find that the two ICESat-2-derived data sets, TCarta and SDBED, that use machine learning depth-detection approaches perform almost identically in predicting inland flood extents and impacts. The ACA, which uses a physics-based attenuation approach (Li et al., 2019), generally estimates lower depths in both lagoons. This results in a relative under-prediction of flood extents in the shallow northern shelf lagoon and a relative over-prediction of flood extents in the deeper central shelf lagoon. The similarity in peak flood heights between the two ICESat-2 data sets, one of which is limited to a depth of ~20 m, also suggests that water depths more than 20 m may not influence onshore flooding for this track and northern location, though southern sensitivities could vary with different storm paths. Despite the minimal impact of onshore flooding, depths beyond 20 m continue to matter for peak wave heights (Jackson et al., 2022; Khanarmuei et al., 2020), underlining the advantage of our approach integrating locally available nautical charts and other depth data.

Our study presents a novel exploration of how spatially varying vertical bathymetric uncertainty propagated through the flood model affects peak flood heights, wave heights, and inundation extent. A unique feature of the new SDBED data set is the information on the uncertainty value per pixel for the satellite-derived and slope profile components of the bathymetry. Publicly available bathymetry data sets used in flood modeling typically do not provide information on spatially varying uncertainties. The globally available GEBCO bathymetry data set has a spatial resolution of ~460 m with no information provided on spatially varying uncertainties (Jackson et al., 2022; Khanarmuei et al., 2020). The other publicly available data sets, TCarta and ACA, report global vertical uncertainties of ~10% with root mean square error ranges between 1.22 and 1.86 m, both outside the tidal ranges of 0.10–0.20 m, in these lagoons (ESRI, 2025; Li et al., 2019). When these vertical uncertainties exceed the tidal range, as is the case with TCarta and ACA in Belize, it is likely that the effect of vertical uncertainties can cause significant over- or under-prediction in modeled flood extents. Consequently, the influence of these variations on predicted inundation requires careful investigation to ensure reliable modeling in such environments (Blain et al., 1998).

With SDBED, we also present a transferable approach to augment satellite-derived bathymetry data sets using the optical characteristics of the coastal margins. By mapping the optical characteristics of the coastal margins, we identify locations best suited for the Satellite-Derived Bathymetry (SDB) and locations where alternative data are needed. The major limitation of SDB data sets is water clarity (Caballero & Stumpf, 2023), which, in our approach, limits both the acquisition of ICESat-2 training data and quality optical satellite data on which to develop bathymetric models. While we do not ground-truth the depth estimates for SDBED, our use of ancillary depth data from published nautical charts and reef slope data allows us to fill data gaps in the complex Belize coastal zone that cannot be filled using satellite-derived data alone. We do not compare the quality of depth estimates between SDBED and the other three data sets, while noting that the ACA and free version of TCarta are both limited in their coverage, for example, outside the coral reef areas for ACA and within the lagoon for both data sets. In contrast, our hybridized approach allows for the use of satellite-derived bathymetry augmented with additional locally available high-resolution data. Our SDBED workflow is open source, from bathymetry delineation to machine learning prediction. Recent adjustments to the ICESat-2 receiver are expected to result in more and higher-quality bathymetry data, and a NASA-funded data product has been released (Dietrich et al., 2024).

Our findings suggest a qualitative difference between SDBED and GEBCO in the estimates of the population exposed to flooding. The estimates of exposed population are higher for SDBED compared to the estimates with GEBCO bathymetry. Comparisons of the 100 m SDBED with a resampled 460 m SDBED and the 460 m GEBCO data sets (Figure 7) suggest that these differences are likely driven not just by differences in spatial resolution but also by differences in underlying methodologies and data sources. The resampled 460 m SDBED captures key nearshore reef barrier and channel features that are not resolved in GEBCO. Differences in estimating the depths of critical nearshore features also influence variations in population exposed to flooding between SDBED, TCarta, and ACA (Figure 6). The ACA bathymetry, which estimates shallower lagoon depths relative to SDBED and TCarta in the northern shelf lagoon, results in a relative under-prediction of ~10,000 people flooded based on the WorldPop 2020 population data set. On the other hand, differences in estimates of people flooded based on WorldPop 2020 are ~400 people between SDBED and TCarta, which are identical in their estimated depths in the northern shelf lagoon. Differences in bathymetry that propagate to variability in flood impact estimates are critical though difficult to evaluate (Vousdoukas et al., 2018), and our findings show that consideration of these uncertainties is important for estimating flood impacts.

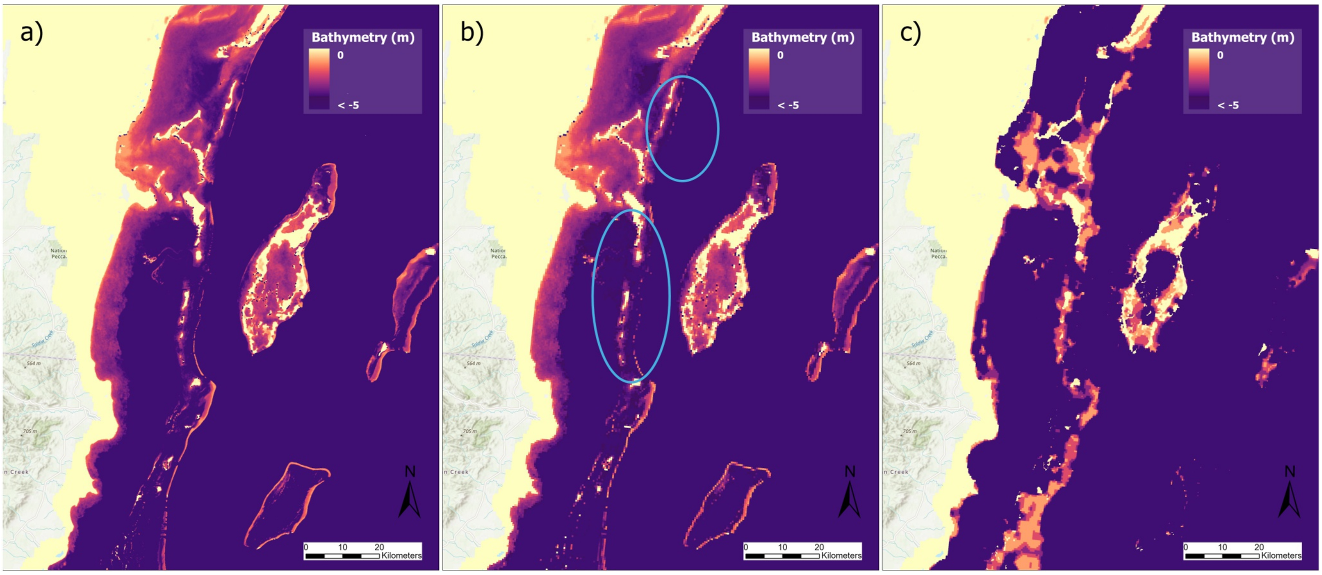

Figure 7. Bathymetric map of the Northern and Central lagoons of Belize shows the differences between the data quality and spatial resolutions. (a) SDBED data set with 100 m, (b) SDBED resampled to 460 m, and (c) GEBCO data set with 460 m spatial resolutions. The blue circles in panel (b) highlight the absence of some nearshore features (barrier reefs) due to the low resolution of the data set and the size of those features.

This study reveals the importance of accurately estimating depths in coastal lagoon systems for future predictions of flood impacts from storm waves and surges. As storm surge impacts become aggravated by accelerated coastal development, rising sea levels, and the potential intensification of storms, the availability of reliable storm impact models is crucial, especially for lagoon-fronted coastlines (Anthony et al., 2009). Based on these findings, we suggest that storm surge impact predictions for lagoon-fronted coastlines use multiple bathymetry data sets or incorporate vertical uncertainties, as done here with the new SDBED data set, to better describe the possible range of expected impacts. Our study investigates the effect of these uncertainties for one storm and is validated using available water level observations for two historic storms, and further exploration across multiple storms will improve our understanding of the sensitivity of flood impact estimates to these uncertainties. When specific uncertainty information is unavailable, conducting constrained bathymetric sensitivity analyses, for example, considering variations of ± 1 m, can help capture the potential range of storm impact estimates. Additionally, we make our bathymetry data set for Belize and our approach for deriving this data set publicly available (Lagomasino et al., 2025, 2026) for use in future studies exploring wave and water level transformation over coral reef habitats, habitat distribution modeling for seagrass, or the modeling of riverine and sedimentary flows as driving conditions for ecological and geomorphological processes along a lagoon-fronted coastline (Roelfsema et al., 2021).

Conflict of Interest

The authors declare no conflicts of interest relevant to this study.

Data Availability Statement

The bathymetry data set generated in this paper is available online on a Zenodo repository (Lagomasino et al., 2025 [Dataset]). This data set includes three bathymetries: the original SDBED, SDBED-, and SDBED+.

Acknowledgments

Funding for this work was provided under award number 80NSSC23K0130 from the National Aeronautics and Space Administration. The statements, findings, conclusions, and recommendations are those of the authors and do not necessarily reflect the views of the National Aeronautics and Space Administration or East Carolina University.

References

Al-Attabi, Z., Xu, Y., Tso, G., & Narayan, S. (2023). The impacts of tidal wetland loss and coastal development on storm surge damages to people and property: A Hurricane Ike case-study. *Scientific Reports*, *13*(1), 4620. https://doi.org/10.1038/s41598-023-31409-x

Amrari, S., Bourassin, E., Andréfouët, S., Soulard, B., Lemonnier, H., & Le Gendre, R. (2021). Shallow water bathymetry retrieval using a band-optimization iterative approach: Application to New Caledonia coral reef lagoons using Sentinel-2 data. *Remote Sensing*, *13*(20), 4108. https://doi.org/10.3390/rs13204108

Anthony, A., Atwood, J., August, P., Byron, C., Cobb, S., Foster, C., et al. (2009). Coastal lagoons and climate change: Ecological and social ramifications in US Atlantic and Gulf coast ecosystems. *Ecology and Society*, *14*(1), art8. https://doi.org/10.5751/es-02719-140108

Barnard, P. L., Erikson, L. H., Foxgrover, A. C., Hart, J. A. F., Limber, P., O'Neill, A. C., et al. (2019). Dynamic flood modeling essential to assess the coastal impacts of climate change. *Scientific Reports*, *9*(1), 4309. https://doi.org/10.1038/s41598-019-40742-z

Beck, M. W., Losada, I. J., Menéndez, P., Reguero, B. G., Díaz-Simal, P., & Fernández, F. (2018). The global flood protection savings provided by coral reefs. *Nature Communications*, *9*(1), 1–9. https://doi.org/10.1038/s41467-018-04568-z

Beddows, P. A., Glover, J. B., Rissolo, D., Carter, A. M., Jaijel, R., Smith, D. M., & Goodman-Tchernov, B. (2016). The Proyecto Costa Escondida: Recent interdisciplinary research in search of freshwater along the North Coast of Quintana Roo, Mexico. *WIREs Water*, *3*(5), 749–761. https://doi.org/10.1002/wat2.1161

Blain, C. A., Westerink, J. J., & LuettichJr, R. A. (1998). Grid convergence studies for the prediction of hurricane storm surge. *International Journal for Numerical Methods in Fluids*, *26*(4), 369–401. https://doi.org/10.1002/(SICI)1097-0363(19980228)26:4<369::AID-FLD624>3.0.CO;2-0

Bondarenko, M., Nieves, J., Stevens, F., Gaughan, A., Tatem, A., & Sorichetta, A. (2020). *wpgpRFPMS: Random Forests population modelling R scripts, version 0.1. 0*. University of Southampton.

Booij, N., Ris, R. C., & Holthuijsen, L. H. (1999). A third-generation wave model for coastal regions: 1. Model description and validation. *Journal of Geophysical Research*, *104*(C4), 7649–7666. https://doi.org/10.1029/98JC02622

Caballero, I., & Stumpf, R. P. (2023). Confronting turbidity, the major challenge for satellite-derived coastal bathymetry. *Science of the Total Environment*, *870*, 161898. https://doi.org/10.1016/j.scitotenv.2023.161898

Carrasco, A. R., Ferreira, Ó., & Roelvink, D. (2016). Coastal lagoons and rising sea level: A review. *Earth-Science Reviews*, *154*, 356–368. https://doi.org/10.1016/j.earscirev.2015.11.007

Carrasquilla-Henao, M., Rueda, M., & Juanes, F. (2022). Fish habitat use in a Caribbean mangrove lagoon system. *Estuarine, Coastal and Shelf Science*, *278*, 108090. https://doi.org/10.1016/j.ecss.2022.108090

Coluzzi, R., Imbrenda, V., Lanfredi, M., & Simoniello, T. (2018). A first assessment of the Sentinel-2 Level 1-C cloud mask product to support informed surface analyses. *Remote Sensing of Environment*, *217*, 426–443. https://doi.org/10.1016/j.rse.2018.08.009

Dietrich, J. T., Rackley Reese, A., Gibbons, A., Magruder, L. A., & Parrish, C. E. (2024). Analysis of ICESat-2 data acquisition algorithm parameter enhancements to improve worldwide bathymetric coverage. *Earth and Space Science*, *11*(2), e2023EA003270. https://doi.org/10.1029/2023EA003270

Dilmen, D. I., Roe, G. H., Wei, Y., & Titov, V. V. (2018). The role of near-shore bathymetry during tsunami inundation in a reef island setting: A case study of Tutuila Island. *Pure and Applied Geophysics*, *175*(4), 1239–1256. https://doi.org/10.1007/s00024-018-1769-1

Dullaart, J. C., Muis, S., Bloemendaal, N., Chertova, M. V., Couasnon, A., & Aerts, J. C. (2021). Accounting for tropical cyclones more than doubles the global population exposed to low-probability coastal flooding. *Communications Earth & Environment*, *2*(1), 135. https://doi.org/10.1038/s43247-021-00204-9

Dunn, G. E. (1962). The hurricane season of 1961. *Monthly Weather Review*, *90*(3), 107–119. https://doi.org/10.1175/1520-0493(1962)090<0107:thso>2.0.co;2

Egbert, G. D., & Erofeeva, S. Y. (2002). Efficient inverse modeling of barotropic ocean tides. *Journal of Atmospheric and Oceanic Technology*, *19*(2), 183–204. https://doi.org/10.1175/1520-0426(2002)019<0183:eimobo>2.0.co;2

ESRI. (2025). TCarta 10 m Satellite Derived Bathymetry. *ESRI*. Retrieved March 2 from Retrieved from https://www.esri.com/en-us/arcgis-marketplace/listing/products/948350597e67483a9d2f8544cea5c1d9

Garces-Ordonez, O., Saldarriaga-Velez, J. F., Espinosa-Diaz, L. F., Canals, M., Sanchez-Vidal, A., & Thiel, M. (2022). A systematic review on microplastic pollution in water, sediments, and organisms from 50 coastal lagoons across the globe. *Environmental Pollution*, *315*, 120366. https://doi.org/10.1016/j.envpol.2022.120366

Gonzalez-De Zayas, R., Barredo Yera, A., Manduca Artiles, M., Lestayo González, J. A., Castillo Sandoval, F. S., & Merino-Ibarra, M. (2021). Trace metals in sediments of seven coastal lagoons of the Sabana–Camagüey Archipelago, Cuba. *Soil and Sediment Contamination: International Journal*, *30*(3), 331–349.

Gou, X., Liang, H., Cai, T., Wang, X., Chen, Y., & Xia, X. (2023). The impact of coastline and bathymetry changes on the storm tides in Zhejiang coasts. *Journal of Marine Science and Engineering*, *11*(9), 1832. https://doi.org/10.3390/jmse11091832

Gress, E., Voss, J. D., Eckert, R. J., Rowlands, G., & Andradi-Brown, D. A. (2019). The mesoamerican reef. *Mesophotic coral ecosystems*, 71–84.

Harris, D. L., Rovere, A., Casella, E., Power, H., Canavesio, R., Collin, A., et al. (2018). Coral reef structural complexity provides important coastal protection from waves under rising sea levels. *Science Advances*, *4*(2), eaao4350. https://doi.org/10.1126/sciadv.aao4350

Hersbach, H., Bell, B., Berrisford, P., Hirahara, S., Horányi, A., Muñoz-Sabater, J., et al. (2020). The ERA5 global reanalysis. *Quarterly Journal of the Royal Meteorological Society*, *146*(730), 1999–2049. https://doi.org/10.1002/qj.3803

Holthuijsen, L. H. (2010). *Waves in oceanic and coastal waters*. Cambridge University Press. https://doi.org/10.1017/CBO9780511618536

Hsiao, Y.-S., Hwang, C., Cheng, Y.-S., Chen, L.-C., Hsu, H.-J., Tsai, J.-H., et al. (2016). High-resolution depth and coastline over major atolls of South China Sea from satellite altimetry and imagery. *Remote Sensing of Environment*, *176*, 69–83. https://doi.org/10.1016/j.rse.2016.01.016

Jackson, D. W., Short, A. D., Loureiro, C., & Cooper, J. A. G. (2022). Beach morphodynamic classification using high-resolution nearshore bathymetry and process-based wave modelling. *Estuarine, Coastal and Shelf Science*, *268*, 107812. https://doi.org/10.1016/j.ecss.2022.107812

Jing, R., Heft-Neal, S., Chavas, D. R., Griswold, M., Wang, Z., Clark-Ginsberg, A., et al. (2024). Global population profile of tropical cyclone exposure from 2002 to 2019. *Nature*, *626*(7999), 549–554. https://doi.org/10.1038/s41586-023-06963-z

Kennish, M. J., & Paerl, H. W. (2010). *Coastal lagoons: Critical habitats of environmental change*. CRC Press.

Khanarmuei, M., Suara, K., Sumihar, J., & Brown, R. J. (2020). Hydrodynamic modelling and model sensitivities to bed roughness and bathymetry offset in a micro-tidal estuary. *Journal of Hydroinformatics*, *22*(6), 1536–1553. https://doi.org/10.2166/hydro.2020.102

Kjerfve, B. (1994). Coastal lagoons. In *Elsevier oceanography series* (Vol. 60, pp. 1–8). Elsevier. https://doi.org/10.1016/s0422-9894(08)70006-0.Elsevier Oceanography Series.

Kjerfve, B., & Magill, K. E. (1989). Geographic and hydrodynamic characteristics of shallow coastal lagoons. *Marine Geology*, *88*(3), 187–199. https://doi.org/10.1016/0025-3227(89)90097-2

Knutson, T., Camargo, S. J., Chan, J. C., Emanuel, K., Ho, C.-H., Kossin, J., et al. (2020). Tropical cyclones and climate change assessment: Part II: Projected response to anthropogenic warming. *Bulletin of the American Meteorological Society*, *101*(3), E303–E322. https://doi.org/10.1175/BAMS-D-18-0194.1

Kobara, S., & Heyman, W. D. (2010). Sea bottom geomorphology of multi-species spawning aggregation sites in Belize. *Marine Ecology Progress Series*, *405*, 243–254. https://doi.org/10.3354/meps08512

Krichene, H., Vogt, T., Piontek, F., Geiger, T., Schötz, C., & Otto, C. (2023). The social costs of tropical cyclones. *Nature Communications*, *14*(1), 7294. https://doi.org/10.1038/s41467-023-43114-4

Lagomasino, D., Babanawo, D., Al-Attabi, Z., Narayan, S., Campbell, A., Wuppukondur, A., et al. (2025). Satellite-Derived bathymetry (SDBED) for Belize [Dataset]. *Zenodo*. https://doi.org/10.5281/zenodo.17525111

Lagomasino, D., Babanawo, D., & Moreno, S. (2026). An integrated remote sensing and machine learning framework for coastal Margin classification and shallow-water bathymetry. *Zenodo*, *1*. https://doi.org/10.5281/zenodo.18350940

Li, J., Knapp, D. E., Schill, S. R., Roelfsema, C., Phinn, S., Silman, M., et al. (2019). Adaptive bathymetry estimation for shallow coastal waters using Planet Dove satellites. *Remote Sensing of Environment*, *232*, 111302. https://doi.org/10.1016/j.rse.2019.111302

Liu, L., Cao, X., Li, S., & Jie, N. (2024). A 31-year (1990–2020) global gridded population dataset generated by cluster analysis and statistical learning. *Scientific Data*, *11*(1), 124. https://doi.org/10.1038/s41597-024-02913-0

Lorenz, M., Arns, A., & Gräwe, U. (2023). How Sea level rise May hit you through the backdoor: Changing extreme water levels in shallow coastal Lagoons. *Geophysical Research Letters*, *50*(21), e2023GL105512. https://doi.org/10.1029/2023GL105512

Lowe, R. J., Hart, C., & Pattiaratchi, C. B. (2010). Morphological constraints to wave-driven circulation in coastal reef-lagoon systems: A numerical study. *Journal of Geophysical Research*, *115*(C9). https://doi.org/10.1029/2009JC005753

Lyons, M. B., Murray, N. J., Kennedy, E. V., Kovacs, E. M., Castro-Sanguino, C., Phinn, S. R., et al. (2024). New global area estimates for coral reefs from high-resolution mapping. *Cell Reports Sustainability*, *1*(2), 100015. https://doi.org/10.1016/j.crsus.2024.100015

Martín, A., Amores, A., Orfila, A., Toomey, T., & Marcos, M. (2023). Coastal extreme sea levels in the Caribbean Sea induced by tropical cyclones. *Natural Hazards and Earth System Sciences*, *23*(2), 587–600. https://doi.org/10.5194/nhess-23-587-2023

Mayer, L., Jakobsson, M., Allen, G., Dorschel, B., Falconer, R., Ferrini, V., et al. (2018). The Nippon Foundation—Gebco seabed 2030 project: The quest to see the world's oceans completely mapped by 2030. *Geosciences*, *8*(2), 63. https://doi.org/10.3390/geosciences8020063

McCabe, R. M., Estrade, P., Middleton, J. H., Melville, W. K., Roughan, M., & Lenain, L. (2010). Temperature variability in a shallow, tidally isolated coral reef lagoon. *Journal of Geophysical Research*, *115*(C12). https://doi.org/10.1029/2009JC006023

McNeill, D. F., Janson, X., Bergman, K. L., & Eberli, G. P. (2010). Belize: A modern example of a mixed carbonate-siliciclastic Shelf. In *Carbonate depositional systems: Assessing dimensions and controlling parameters: The Bahamas, Belize and the Persian/Arabian Gulf* (pp. 81–143). Springer. https://doi.org/10.1007/978-90-481-9364-6_3

Menéndez, P., Losada, I. J., Torres-Ortega, S., Narayan, S., & Beck, M. W. (2020). The global flood protection benefits of mangroves. *Scientific Reports*, *10*(1), 1–11. https://doi.org/10.1038/s41598-020-61136-6

Nancoo, M. E. (1962). Hurricane 'HATTIE. *Weather*, *17*(9), 295–304. https://doi.org/10.1002/j.1477-8696.1962.tb07316.x

Parodi, M. U., Giardino, A., Van Dongeren, A., Pearson, S. G., Bricker, J. D., & Reniers, A. J. (2020). Uncertainties in coastal flood risk assessments in small island developing states. *Natural Hazards and Earth System Sciences*, *20*(9), 2397–2414. https://doi.org/10.5194/nhess-20-2397-2020

Paugam, C., Sous, D., Rey, V., Meulé, S., Faure, V., Boutron, O., et al. (2021). Wind tides and surface friction coefficient in semi-enclosed shallow lagoons. *Estuarine, Coastal and Shelf Science*, *257*, 107406. https://doi.org/10.1016/j.ecss.2021.107406

Reguero, B. G., Losada, I. J., Díaz-Simal, P., Méndez, F. J., & Beck, M. W. (2015). Effects of climate change on exposure to coastal flooding in Latin America and the Caribbean. *PLoS One*, *10*(7), e0133409. https://doi.org/10.1371/journal.pone.0133409

Reguero, B. G., Storlazzi, C. D., Gibbs, A. E., Shope, J. B., Cole, A. D., Cumming, K. A., & Beck, M. W. (2021). The value of US coral reefs for flood risk reduction. *Nature Sustainability*, *4*(8), 688–698. https://doi.org/10.1038/s41893-021-00706-6

Ris, R., Holthuijsen, L., & Booij, N. (1999). A third-generation wave model for coastal regions: 2. Verification. *Journal of Geophysical Research*, *104*(C4), 7667–7681. https://doi.org/10.1029/1998JC900123

Rodrigues-Filho, J. L., Macêdo, R. L., Sarmento, H., Pimenta, V. R. A., Alonso, C., Teixeira, C. R., et al. (2023). From ecological functions to ecosystem services: Linking coastal lagoons biodiversity with human well-being. *Hydrobiologia*, *850*(12), 2611–2653. https://doi.org/10.1007/s10750-023-05171-0

Roelfsema, C. M., Lyons, M. B., Castro-Sanguino, C., Kovacs, E. M., Callaghan, D., Wettle, M., et al. (2021). How much shallow coral habitat is there on the Great Barrier Reef? *Remote Sensing*, *13*(21), 4343. https://doi.org/10.3390/rs13214343

Sampson, C. C., Smith, A. M., Bates, P. D., Neal, J. C., & Trigg, M. A. (2016). Perspectives on open access high resolution digital elevation models to produce global flood hazard layers. *Frontiers in Earth Science*, *3*, 85. https://doi.org/10.3389/feart.2015.00085

Serafin, K. A., Ruggiero, P., Barnard, P. L., & Stockdon, H. F. (2019). The influence of shelf bathymetry and beach topography on extreme total water levels: Linking large-scale changes of the wave climate to local coastal hazards. *Coastal Engineering*, *150*, 1–17. https://doi.org/10.1016/j.coastaleng.2019.03.012

The icepyx Developers. (2023). Python tools for obtaining and working with ICESat-2 data. https://doi.org/10.5281/zenodo.7729175

Thomas, N., Lee, B., Coutts, O., Bunting, P., Lagomasino, D., & Fatoyinbo, L. (2022). A purely spaceborne open source approach for regional bathymetry mapping. *IEEE Transactions on Geoscience and Remote Sensing*, *60*, 1–9. https://doi.org/10.1109/TGRS.2022.3192825

Traganos, D., Aggarwal, B., Poursanidis, D., Topouzelis, K., Chrysoulakis, N., & Reinartz, P. (2018). Towards global-scale seagrass mapping and monitoring using Sentinel-2 on Google Earth engine: The case Study of the Aegean and Ionian Seas. *Remote Sensing*, *10*(8), 1227. https://doi.org/10.3390/rs10081227

Vousdoukas, M. I., Bouziotas, D., Giardino, A., Bouwer, L. M., Mentaschi, L., Voukouvalas, E., & Feyen, L. (2018). Understanding epistemic uncertainty in large-scale coastal flood risk assessment for present and future climates. *Natural Hazards and Earth System Sciences*, *18*(8), 2127–2142. https://doi.org/10.5194/nhess-18-2127-2018

Warszawski, L., Frieler, K., Huber, V., Piontek, F., Serdeczny, O., Zhang, X., et al. (2017). *Center for international earth science information network—ciesin—columbia university.(2016). gridded population of the world, version 4 (gpwv4): Population density. palisades*. Nasa socioeconomic data and applications center (sedac). Atlas of Environmental Risks Facing China Under Climate Change. https://doi.org/10.7927/h4np22dq.228.

Weaver, R., & Slinn, D. (2010). Influence of bathymetric fluctuations on coastal storm surge. *Coastal Engineering*, *57*(1), 62–70. https://doi.org/10.1016/j.coastaleng.2009.09.012

Zanaga, D., Van De Kerchove, R., Daems, D., De Keersmaecker, W., Brockmann, C., Kirches, G., et al. (2022). ESA WorldCover 10 m 2021 v200.

Zhang, K., Liu, H., Li, Y., Xu, H., Shen, J., Rhome, J., & SmithIII, T. J. (2012). The role of mangroves in attenuating storm surges. *Estuarine, Coastal and Shelf Science*, *102*, 11–23. https://doi.org/10.1016/j.ecss.2012.02.021